Molecular Crystals and Liquid Crystals Science and Technology. Section A. Molecular Crystals and Liquid Crystals

Publication details, including instructions for authors and subscription information:
http://www.tandfonline.com/loi/gmcl19

Magnetic Phase Transitions in $M^{II}[N(CN)_2]_2$

Carmen R. Kmety [a], Jamie L. Manson [b], Qing-Zhen Huang [c d], Jeffrey W. Lynn [c], Ross W. Erwin [c], Joel S. Miller [b] & Arthur J. Epstein [a e]

[a] Department of Physics, The Ohio State University, Columbus, OH, 43210-1106

[b] Department of Chemistry, University of Utah, Salt Lake City, UT, 84112-0850

[c] NIST Center for Neutron Research, Gaithersburg, MD, 20899

[d] Department of Materials and Nuclear Engineering, University of Maryland, College Park, MD, 20742

[e] Department of Chemistry, The Ohio State University, Columbus, OH, 43210-1106

Version of record first published: 24 Sep 2006

Mol. Cryst. and Liq. Cryst., 1999, Vol. 334, pp. 631-640
Reprints available directly from the publisher
Photocopying permitted by license only

Magnetic Phase Transitions in $M^{II}[N(CN)_2]_2$

CARMEN R. KMETY[a], JAMIE L. MANSON[b], QING-ZHEN HUANG[cd], JEFFREY W. LYNN[c], ROSS W. ERWIN[c], JOEL S. MILLER[b] and ARTHUR J. EPSTEIN[ae]

[a]*Department of Physics, The Ohio State University, Columbus, OH 43210–1106,* [b]*Department of Chemistry, University of Utah, Salt Lake City, UT 84112–0850,* [c]*NIST Center for Neutron Research, Gaithersburg, MD 20899,* [d]*Department of Materials and Nuclear Engineering, University of Maryland, College Park, MD 20742 and* [e]*Department of Chemistry, The Ohio State University, Columbus, OH 43210–1106*

We summarize the magnetic behavior of $M^{II}[N(CN)_2]_2$ (M = Co, Ni, Mn and Zn). Analyses of the DC magnetization and AC susceptibility data demonstrate that α-$Co^{II}[N(CN)_2]_2$ (**1a**) and $Ni^{II}[N(CN)_2]_2$ (**2**) are ferromagnets below T_c, while β-$Co^{II}[N(CN)_2]_2$ (**1b**) and $Mn^{II}[N(CN)_2]_2$ (**3**) are canted antiferromagnets below T_N. $Zn^{II}[N(CN)_2]_2$ (**4**) is diamagnetic. Specific heat and neutron powder diffraction results clearly define the transition temperatures for **1a, 1b, 2** and **3.** Crystal structure determination from high-resolution neutron powder data for **1a, 2** and **3** shows that the three systems are isomorphous and crystallize in the orthorhombic space group *Pnnm* with Z = 2. Single crystal X-ray diffraction shows that **4** crystallizes in the orthorhombic space group *Pnma* with Z = 4. We solved the magnetic structures of **1a, 2** and **3** from neutron powder diffraction experiments. All low-temperature measurements are consistent with high-spin **1b, 2, 3** and **4,** though **1a** exhibits an effective J′ = 1/2 behavior.

Keywords: dicyanamide compounds; canted antiferromagnet; ferromagnet; neutron powder diffraction; specific heat

INTRODUCTION

The dicyanamide compounds $M^{II}[N(CN)_2]_2$ are a new class of molecule-based magnetic materials composed of transition metal ions (M = Co, Ni, Mn and Zn) and C_{2v} organic ligand dicyanamide $[N(CN)_2]^-$[1,2,3,4,5,6,7]. Based on high-resolution neutron powder diffraction (NPD) experiments, **1a**, **2** and **3** crystallize in the orthorhombic space group *Pnnm* (No. 58) with Z = 2 (Fig. 1(a)). The crystal structure consists of planar $M^{II}[N(CN)_2]_2$ chains parallel to the *c*-axis, passing through the corners and the center of the unit cell[2,6]. From single crystal X-ray diffraction analysis, **4** crystallizes in the orthorhombic space group *Pnma* (No. 62) with Z = 4 (Fig. 1(b)). The crystal structure consists of layers of nearly ideal squares of Zn^{II}, parallel to the *ab*-plane[4]. The compounds **1a**, **2** and **3** have an octahedral geometry around the metal ion, while **1b** and **4** have a tetrahedral geometry for the metal ion. DC magnetization and AC susceptibility studies show that **1a** and **2** are ferromagnets below T_C, while **1b** and **3** are canted antiferromagnets below T_N[2,6]. **4** is diamagnetic[4]. Low temperature specific heat measurements of **1a**, **1b**, **2** and **3**, were used to detect the existence of magnetic phase transitions, and to determine the type of spin-spin interaction and the dimensionality of the magnetic lattice[5]. From NPD data, we solved the magnetic structures for **1a**, **2** and **3**[6]. This is the *first* determination of the magnetic structure of a molecule-based magnet from NPD data by finding the best agreement between the experimental and calculated ratios of the integrated intensities of several magnetic Bragg peaks. For the studied compounds, the observed magnetism corresponds to the high-spin state of the M^{II} ions. **1a** has J′ = 1/2 (S = 3/2 and L = 1)[8] at low temperatures that gradually changes to J = 3/2 at high temperatures, which is consistent with the data discussed here. The crystallographic simplicity combined with the richness of the magnetic phenomena makes the dicyanamide compounds ideal model systems for studying the relationship between structure and magnetic properties.

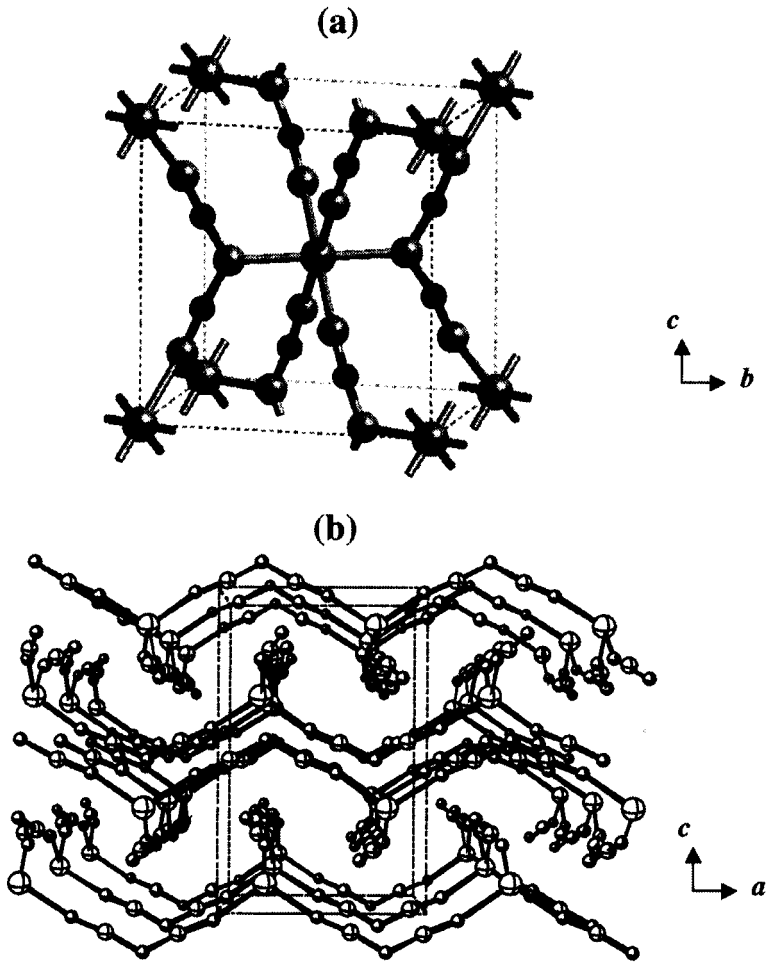

FIGURE 1 Crystal structure for $M^{II}[N(CN)_2]_2$, (a) M = Co (**1a**), Ni (**2**)and Mn (**3**) and (b) M = Zn (**4**). (Figure 1(b) reprinted with permission from ref. [4]. Copyright 1998 American Chemical Society.)

EXPERIMENTAL

The sample preparation is described elsewhere[2,6,7]. DC magnetization data were collected using a Quantum Design MPMS-5 SQUID magnetometer with a continous-flow cryostat and a 5.5 T superconducting solenoid. AC susceptibility data were recorded with a Lake Shore Model 7225 AC susceptometer/DC magnetometer with an exchange cryostat and a 5.0 T superconducting solenoid. Phase-sensitive measurements were made using a lock-in amplifier. The samples used for magnetic measurements were prepared in gelatin capsules in air. The specific heat measurements were performed with a Quantum Design PPMS[9] and the samples were cut from pressed pellets of polycrystalline powders. The NPD measurements were carried out at the National Institute of Standards and Technology (NIST) research reactor. For crystal structure determination, the NPD measurements were made with the 32-detector BT-1 high-resolution powder diffractometer using incident neutron beams of wavelength 1.5401 Å produced by a Cu (311) monochromator. Crystal structures were refined by the Rietveld technique, using the GSAS program[10] and adopting as initial model the structure derived previously[2]. For magnetic structure determination, the NPD experiments were carried out on the BT-2 triple-axis spectrometer utilizing an incident neutron beam with wavelength of 2.3591 Å produced by a pyrolitic graphite (002) monochromator and filter. The polycrystalline samples were sealed in vanadium (BT-1) or aluminum (BT-2) containers filled with He-exchange gas. For **1a**, **1b** and **2** all measurements were performed on samples from the same batches.

RESULTS AND DISCUSSION

The temperature dependence of the DC susceptibility, χ_{DC}, measured in constant applied magnetic field between 2 and 300 K, is presented as $1/\chi_{DC}$ in Fig. 2(a) for **1b** and Fig. 2(b) for **2**. All samples exhibit a linear $1/\chi_{DC}$ vs. T at high temperatures. A fit of the Curie-Weiss law $1/\chi_{DC} = (T-\theta)/C$ to the data in the high T region for each compound gives the intercept with the T axis, θ, and the slope, C^{-1}. For **1a** and **2**, θ is positive suggesting pairwise FM interactions above the ordering temperature. For **1b** and **3**, θ is negative suggesting AFM interactions above the ordering temperature. From the Curie constant we obtain the spin multiplicities and the g-values. The spin multiplicities and the g-values for the compounds studied are: S = 3/2 and g =

2.49[6,11] (**1a**); S = 3/2 and g = 2.27[2] (**1b**); S = 1 and g = 2.21[6,11] (**2**); and S = 5/2 and g = 2.00[6,7] (**3**). Deviations from the Curie-Weiss law were observed at low temperatures, which are due to both exchange interactions and single-ion anisotropy.

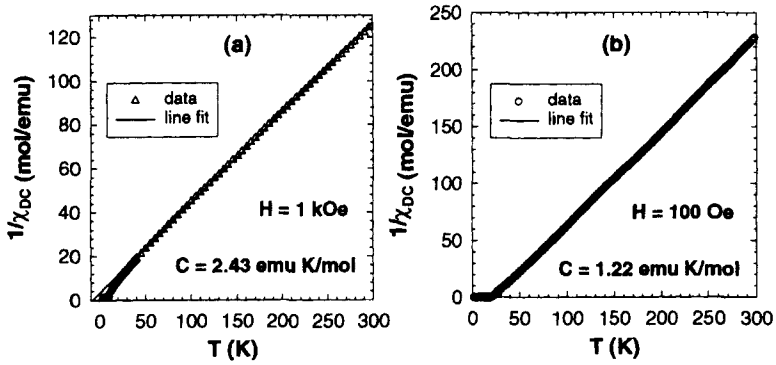

FIGURE 2: $1/\chi_{DC}$ vs. T for $M^{II}[N(CN)_2]_2$, (a) M = Co (**1b**) and (b) M = Ni (**2**). (Figure 2(a) reprinted in part with permission from ref. [2]. Copyright 1998 American Chemical Society.)

The temperature dependence of the DC susceptibility, χ_{DC}, is presented as the $\chi_{DC}T$ product in Fig. 3(a) for **1b** and Fig. 3(b) for **2**. On cooling from room temperature the $\chi_{DC}T$ product for **2** remains nearly constant, then, below 21 K, increases rapidly with a peak around 16 K. This increase of the $\chi_{DC}T$ and the presence of the peak suggest a transition to a FM state. For **1b**, the $\chi_{DC}T$ product first decreases, indicating antiferromagnetic correlations followed by a minimum at 24 K, a very rapid increase as the temperature is lowered further, and a maximum at 7 K. This behavior is associated with a transition to a canted AFM (weak FM) state. Similar $\chi_{DC}T$ versus T data shows that **1a** is a ferromagnet[2,6], while **3** is a canted antiferromagnet[6].

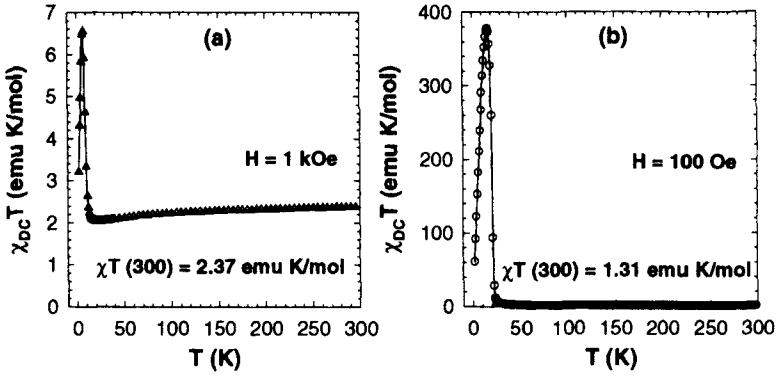

FIGURE 3 $\chi_{DC}T$ versus T for $M^{II}[N(CN)_2]_2$, (a) M = Co (**1b**) and (b) M = Ni (**2**). (Figure 3(a) reprinted in part with permission from ref. [2]. Copyright 1998 American Chemical Society.)

Hysteresis curves at T = 2 K give saturation magnetization[2,6] values of ≈ 14500 and 11900 emu Oe/mol, and coercive fields[2] of 800 and 7000 Oe (samples constrained in epoxy) for **1a** and **2**, respectively. The observed saturation magnetization for **1a** is smaller than the expected ferromagnetic saturation magnetization value of 20860 emu Oe/mol for J = 3/2 and g = 2.49, or even 16755 emu Oe/mol for J = 3/2 and g = 2.00. This experimental saturation magnetization for **1a** corresponds to an effective J′ = 1/2 and g′ = 5.20, which indicates that at low temperatures only the lowest Kramers doublet is thermally populated[8]. The observed saturation magnetization for **2** gives J = 1 and g = 2.13, which corresponds to what is expected if all spins are aligned in one direction. The field dependence of the magnetization for **1b** and **3** is linear, with no saturation of the magnetization at the highest measured field 5.5 T, except in the low field region where a small hysteresis loop with coercive fields of 680 Oe (**1b**)[2] and 766 Oe (**3**)[6] (without epoxy) is present. This shows that the low temperature state for these compounds is a canted AFM state, which is consistent with the temperature dependence of χ_{DC} results.

The field-cooled (FC) and zero-field-cooled (ZFC) magnetization versus temperature plots in various DC fields are presented in Fig. 4(a) for **1b** and Fig. 4(b) for **2**. The FC magnetizations obtained on cooling within the fields

show typical features of ferromagnetic/canted antiferromagnetic transitions. The ZFC magnetizations were obtained by cooling below the transition temperatures in zero field and then applying the fields and warming. The bifurcation temperatures (T_b) defined by the onset of irreversibilities for the samples studied are: 9.4 K (**1a**)[6,12], 9.54 K (**1b**)[2,12], 22.2 K (**2**)[6,12] and 16.0 K (**3**)[6]. For **1a**, **2** and **3** the bifurcation temperatures do not depend on the applied field. This contrasts with expectations for materials exhibiting glassy behavior[13]. We conclude that there is no glassy behavior in these materials, which makes them suitable for low temperature neutron studies.

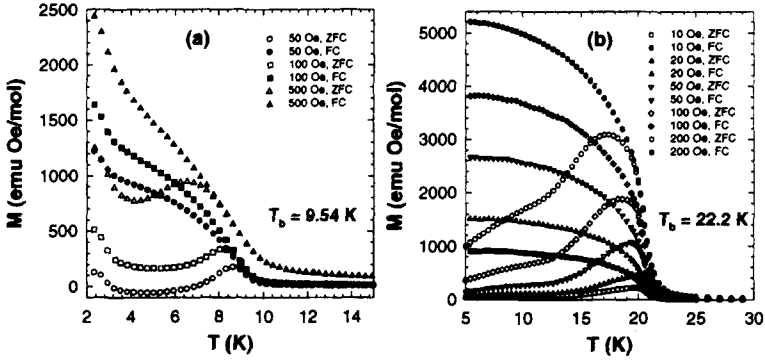

FIGURE 4 FC and ZFC magnetization versus T for $M^{II}[N(CN)_2]_2$, (a) M = Co (**1b**) and (b) M = Ni (**2**). (Figure 4(a) reprinted in part with permission from ref. [2]. Copyright 1998 American Chemical Society.)

The in-phase, χ', and out-of-phase, χ'', components of the complex AC susceptibility as a function of frequency and temperature are presented in Fig. 5(a) for **1b** and Fig. 5(b) for **2**. Both real and imaginary components of the susceptibility show a rather complicated behavior. For **2**, the peak in $\chi'(T)$ at T_p = 20.7 K is accompanied by a shoulder at T_s = 22.2 K. The $\chi''(T)$ follows this structure with a primary peak at T_{p1} = 20.1 K and a weaker peak at T_{p2} = 21.8 K[6]. The peak in χ' is associated with a phase transition from a paramagnetic state to a ferromagnetic state, while the shoulder may be due to the presence of very slow spin-lattice relaxation processes. For **1b**, there are two well-defined peaks in $\chi'(T)$ at T_{p1} = 2.7 and T_{p2} = 8.9 K, and in $\chi''(T)$ at T_{p1}

= 2.5 and T_{p2} = 8.7 K[2]. The presence of two peaks suggests the existence of two phase transitions in this system: first, right below 8.9 K, from a paramagnetic to a canted aniferromagnetic state and second, somewhat below 2.7 K, to another canted antiferromagnetic state of a different angle. The difference between the transition and peak temperatures reflects the presence of short range order above T_N.

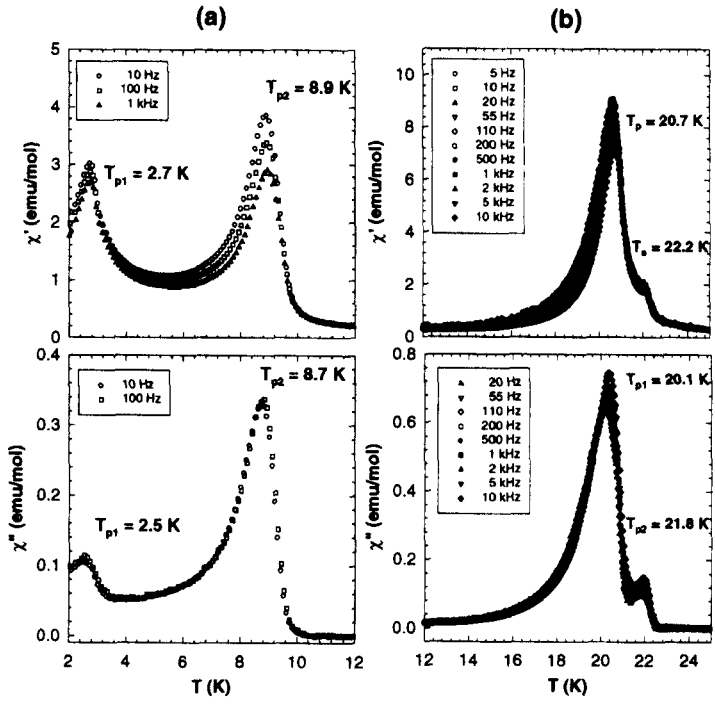

FIGURE 5 In-phase, χ', and out-of-phase, χ'' components of the complex AC susceptibility as a function of temperature and frequency for $M^{II}[N(CN)_2]_2$, (a) M = Co (**1b**) and (b) M = Ni (**2**). (Figure 5(a) reprinted in part with permission from ref. [2]. Copyright 1998 American Chemical Society.)

We performed specific heat measurements[5] with the aim of independent determination of the phase transition temperatures originating in the onset of long-range order. The transition temperatures obtained from specific heat measurements were confirmed by the NPD measurements. In addition, we determined the magnetic lattice, spin direction and the value of the ordered moment per metal ion for **1a**, **2** and **3** from NPD data[6]. The magnetic structures obtained are consistent with all the magnetic and thermal results of the bulk substance.

CONCLUSION

The use of DC magnetization, AC susceptibility, specific heat and NPD techniques, and the analyses of the results provided us with a coherent picture at the macroscopic and microscopic scale for the new class of molecular magnets $M^{II}[N(CN)_2]_2$. We determined the crystal structure (**1a**, **2**, **3** and **4**) and magnetic properties (**1a**, **1b**, **2**, **3** and **4**) for these systems. Our analysis indicates that the crystal structures for **1a**, **2** and **3** are isomorphous and they are described by the orthorombic space group *Pnnm*, while **4** crystallizes in the orthorhombic space group *Pnma*. Our structural results are consistent with the predictions of Koehler and coworkers[1]. **1a** and **2** order ferromagnetically, while **1b** and **3** order as canted antiferromagnets. Depending on the transition metal ion used, similar crystal structures give different magnetic structures: ferromagnetic for **1a** and **2**, versus canted antiferromagnetic for **3**. These results provide a strong basis for understanding the correlations between the crystal structure and magnetic properties of $M^{II}[N(CN)_2]_2$ compounds.

Acknowledgments

This work was supported in part by the U. S. Department of Energy, Division of Material Science, Grant Nos. DE-FG02-86BR45271 and DE-FG03-93ER45504, and the U. S. National Science Foundation, Grant No. DMR95-01325. We thank R. Black and J. Diederichs (Quantum Design, San Diego, CA) for acquiring the specific heat data. Identification of commercial equipment in the text is not intended to imply recommendation or endorsement by the National Institute of Standards and Technology.

References

[1] H. Koehler, A. Kolbe and G. Lux, *Z. Anorg. Allg. Chem.*, **428,** 103 (1977).

[2] J.L. Manson, C.R. Kmety, Q. Huang, J.W. Lynn, G.M. Bendele, S. Pagola, P.W. Stephens, L.M. Liable-Sands, A.L. Rheingold, A.J. Epstein and J.S. Miller, *Chem. Mater.*, **10,** 2552 (1998)..

[3] S.R. Batten, P. Jensen, B. Moubaraki, K.S. Murray and R. Robson, *Chem. Commun.*, 439 (1998).

[4] J.L. Manson, D.W. Lee, A.L. Rheingold and J.S. Miller, *Inorg. Chem.*, **37,** 5966 (1998).

[5] C.R. Kmety, J.L. Manson, J.S. Miller and A.J. Epstein, to be published.
[6] C.R. Kmety, J.L. Manson, Q. Huang, J.W. Lynn, R.W. Erwin, J.S. Miller and A.J. Epstein, to be published.
[7] J.L. Manson, J.S. Miller, submitted.
[8] R.L. Carlin, *Magnetochemistry* (Springer-Verlag, New York, 1986), Chap. 2; W.K. Robinson and S.A. Friedberg, *Physical Review* **117**,402 (1960).
[9] Quantum Design Inc., San Diego, California.
[10] A.C. Larson and R.B. Von Dreele, *General Structure Analysis System,*Los Alamos National Laboratory Report No. LAUR-86–748, (1990).
[11] The g values are slightly different from the values reported in ref. [2] for data acquired on different batches using different experimental facilities, and for different fitting ranges.
[12] The T_b values are slightly different than the values reported in ref [2], due to choice of criteria for analysis and/or different experimental facilities and/or different batches used.
[13] J.A. Mydosh, *Spin Glasses: An Experimental Introduction* (Taylor and Francis, London, 1993).